Chin. Geogra. Sci. 2022 Vol. 32 No. 4 pp. 563−579
https://doi.org/10.1007/s11769-022-1286-0

Springer Science Press
www.springerlink.com/content/1002-0063

Variation in Short-term Temperature Fluctuations Across China During the Past 60 Years

HE Yunchuan[1, 2], DENG Jianming[1], ZHANG Yunlin[1], DING Yanqing[2], QIN Boqiang[1]

(1. *Taihu Lake Laboratory Ecosystem Research Station*, *State Key Laboratory of Lake Science and Environment*, *Nanjing Institute of Geography and Limnology*, *Chinese Academy of Sciences*, *Nanjing* 210008, *China*; 2. *School of Resource and Geosciences*, *China University of Mining and Technology*, *Xuzhou* 221116, *China*)

Abstract: Short-term temperature fluctuations (STFs), including amplitude and frequency fluctuations, are one of the main features of weather and play vital roles in determining the type of ecosystem present. Although temperature fluctuations at different time scales have been extensively discussed, the research on week-scale STFs is lacking. In this study, we developed a method, that can quantify the amplitude and frequency of STFs by the thresholds from all years. We used this method to quantify the amplitude and frequency of the 7-d STFs from 1951 to 2019 across China. Our results indicate that the amplitude of the STF was much higher in the eastern part of China than in the western part, while the frequency of the STF was higher in the middle part than in the southern and northern parts; furthermore, the STF was highly dependent on internal factors such as topography. The long-term STF mainly showed a decreasing trend before 1990, which implies that temperature became increasingly stable from the 1950s to the 1990s. The main influencing factors were related to topography since the trends were relatively consistent in space. A case study in Taihu Lake showed that an unstable STF in winter and summer resulted in a smaller bloom area in the following spring and autumn. Our method could eliminate seasonal effects and is capable of analyzing STFs at scales ranging from days to years. Quantifications of the amplitude and frequency also make the STF indicators more comprehensive. Furthermore, the STF increased significantly across most of China after 1990, which implies that temperature is becoming increasingly unstable. The drivers of these STFs are related to human impacts since the trends are different in space.

Keywords: short-term temperature fluctuation; altitude effect; global warming; climate change; China

Citation: HE Yunchuan, DENG Jianming, ZHANG Yunlin, DING Yanqing, QIN Boqiang, 2022. Variation in Short-term Temperature Fluctuations Across China During the Past 60 Years. *Chinese Geographical Science*, 32(4): 563−579. https://doi.org/10.1007/s11769-022-1286-0

1 Introduction

Global warming has been widely reported (IPCC, 2021). This warming trend has impacts on different ecosystems, e.g., warming promotes cyanobacterial blooms in freshwater lakes. In addition to global warming, short-term temperature fluctuations (STFs), e.g., temperature variation during a week, have many ecological impacts over diverse time scales, and they closely affect the acting patterns of features. At the minute level, temperature fluctuations can affect isoprene emission from leaves (Singsaas and Sharkey, 1998). The capability of the anaerobic biomass is sensitive to temperature fluctuations within hours, and temperature fluctuations influ-

Received date: 2021-06-18; accepted date: 2021-11-18
Foundation item: Under the auspices of the National Natural Science Foundation of China (No. 41971146, 41621002), the Fundamental Research Funds for the Central Universities (No. 2014QNA86), the National Key Research and Development Program of China (No. 2019YFC1805400)
Corresponding author: DENG Jianming. E-mail: jmdeng@niglas.ac.cn

ence the anaerobic digestion process, which affects both biochemical and physical reactions (Peces et al., 2013). The amplitude of the daily temperature fluctuation changes in seasons helps to explain the seasonal forcing of dengue virus transmission in locations where the average temperature does not vary seasonally and mosquito abundance is not associated with dengue incidence (Lambrechts et al., 2011). Temperature fluctuations in weeks during incubation may have substantial effects on reptile populations (Shine and Elphick, 2001). The influenza epidemic, a popular topic, can be attributed to temperature fluctuations at the seasonal scale. From historical data, large rapid temperature fluctuations in autumn can be observed as preconditions of the deadly influenza epidemic in the subsequent months in the highly populated northern mid-latitudes; one example is a typical case of the influenza epidemic season from 2017–2018 (Liu et al., 2020).

Currently, several methods are applied to STF analyses. The diurnal temperature range (DTR), which is a relatively short temporal variation, can greatly influence species distribution (Chan et al., 2016). The DTR is defined as the range enclosed by the daily maximum and minimum temperatures and is a key indicator that provides more information than the mean temperature in determining the effect of climate change (Braganza et al., 2004; Jang et al., 2022). The DTR emphasizes diurnal temperature variations and overlooks temperature differences in consecutive days. The absolute value of the temperature difference between two consecutive days is also an indicator used to reflect sudden temperature variation (Karl et al., 1995) and has been identified as an independent risk factor for human health by small-scale studies (Zhan et al., 2017). This indicator emphasizes sudden temperature variation and is greatly affected by climate patterns changing with seasons. Daily temperature extremes, such as abnormal temperature values that are screened out from standard deviations (Chen et al., 2019), reflect how temperature varies holistically after excluding seasonal effects. Some methods, such as ensemble empirical mode decomposition (EEMD), decompose daily temperature series to obtain intraseasonal weather fluctuations to exclude seasonal effects (Qian et al., 2011; Yin et al., 2017) and quantify temperature fluctuations in a seasonal range. Theses seasonal range methods take seasonal climate changes into consideration, but they can hardly distinguish different time scales of several days or weeks of temperature fluctuations. Among the methods, few of them can take into account the setting of research duration and the elimination of seasonal effects on the basis of quantitative STF amplitude and frequency.

In this study, we develop a method that can quantify the frequency and amplitude of STFs in a 7-d range, which is the typical time scale for weather changes and is commonly referred to as the 'general weather regime' (Eichner et al., 2003). We also estimate the long-term trends of STF frequency and amplitude in China from 1951 to 2019. We use our newly introduced method for the following advantages: 1) custom fluctuation range settings (from days to a year) are accepted after excluding any periodicity effect; and 2) both the amplitude and frequency of fluctuation can be quantified. In this work, we analyze some factors that might contribute to long-term variations in STFs in an attempt to determine the potential drivers.

The ecological effects of climate variations are always the focus of attention, while phytoplankton, as the primary productivity and foundation of the food chain, play an important role in the material circulation and energy transfer processes and reflect the basic status and influence the structure and function of aquatic ecosystems (Kilham, 1987; Meis et al., 2009; Salmaso et al., 2015). Phytoplankton blooms are often used as important indicators to detect the environmental factors and water quality variables in aquatic ecosystems (Cao et al., 2018; Sulastri et al., 2019); therefore, we utilize the phytoplankton bloom area data in a large eutrophic lake (Taihu Lake) to couple the ecosystem and STFs. More specifically, the purposes of this study include determining 1) the spatial and seasonal distributions of the STF pattern across China; 2) the long-term trends of STFs in China; 3) the potential drivers of long-term STF trends; and 4) the ecological effects of STFs.

2 Data and Methods

2.1 Data sources

The climate data including daily temperatures were obtained from the China Meteorological Data Service Center (http://data.cma.cn/). In total, 712 stations (excluding Taiwan due to data unavailable) in China (Fig. 1) with reliable and relatively complete temperature data and analysis were chosen to extract the daily maximum

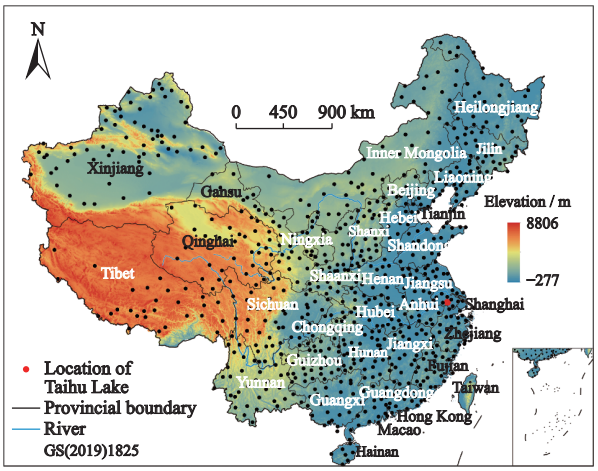

Fig. 1 Meteorology stations (data excluding Taiwan) and the digital elevation model in China and location of Taihu Lake

temperature. The temperature series from these stations have different start years other than 1951, but most series end in 2019. The number of missing data was relatively small (9.51%) and had little impact on the results. The elevation data were from the CGIAR Consortium for Spatial Information (CGIAR-CSI; http://srtm.csi.cgiar.org).

2.2 Quantification of the STF

Although the daily minimum and average temperatures fluctuate in a manner similar to the maximum temperature, we analyzed the maximum temperature to show the STF. The STF was calculated from the temperature difference between any two days in a week.

Our new method can estimate both the STF amplitude and frequency of the fluctuation in a specific time period (e.g., a month, season, or year).

Specifically, we first calculated the difference between T_1 and T_{2-7} for each day:

$$\Delta T_1 = T_{i+1} - T_1 (i = 1,2,3,\ldots,6) \quad (1)$$

where T_1 is the temperature of day 1, i corresponds to the number of days, T_{i+1} is the temperature of day $i+1$, and ΔT_i is the temperature difference between day 1 and day $i+1$. Each day has 6 ΔT_i values; thus, we have ΔT_{1-6} series for each day in a year. For example, ΔT_1 of the same date in each year can form a ΔT_1 series. We then set two threshold values, namely, $h1_{0.05}$, the 5% quantile of the ΔT_1 series, and $h1_{0.95}$, the 95% quantile of the ΔT_1 series. In this way, we obtain $hi_{0.05}$ ($hi_{0.05} < 0$, $i = 1, 2, 3, \ldots, 6$) and $hi_{0.95}$ ($hi_{0.95} > 0$, $i = 1, 2, 3, \ldots, 6$) for each ΔT_i series.

We already have $hi_{0.05}$ and $hi_{0.95}$, and it is possible to judge the ΔT_i of each day by comparing it with $hi_{0.05}$ and $hi_{0.95}$. Starting from ΔT_1, if $\Delta T_1 < h1_{0.05}$ or $\Delta T_1 > h1_{0.95}$, then we mark it as a 'fluctuation day' and regard ΔT_1 as the fluctuation amplitude value of this day, which is designated as FA_d. If $h1_{0.05} < \Delta T_1 < h1_{0.95}$, then we go to the next temperature difference ΔT_2. If $\Delta T_2 < h2_{0.05}$ or $\Delta T_2 > h2_{0.95}$, then the day is marked as a 'fluctuation day', and ΔT_2 is regarded as the FA_d value of this day; otherwise, we go to ΔT_3. A round of calculations for one day ends as follows: 1) at the first $\Delta T_i < hi_{0.05}$ or $\Delta T_i > hi_{0.95}$ occurrence; and 2) when the ΔT_{1-6} are all between $hi_{0.05}$ and $hi_{0.95}$, which means that this day is not a 'fluctuation day', and we set its FA_d value as 0. The calculation flow chart is shown in Appendix hown in Appendix Fig. S1.

The mean monthly fluctuation day was calculated and used as the fluctuation frequency (FF) of each season:

$$FF = N(FA_d)/3 \quad (2)$$

where FF is the seasonal STF fluctuation frequency, and $N(FA_d)$ is the number of days that are 'fluctuation days' in a season.

The monthly average of FA_d in a season was used as the fluctuation amplitude (FA) of this season:

$$FA = \sum |FA_d|/3 \quad (3)$$

where FA is the seasonal STF fluctuation amplitude, and $\sum|FA_d|$ is the sum of the fluctuation amplitude absolute values in a season.

The trends of FF and FA were estimated by the Mann-Kendall trend analysis as τ values by the Mannkendall function in the 'kendall' package in R (R Core Team, 2020).

2.3 Subsequent processing of STF results

Altitude is an important factor in climate patterns. Our hypothesis suggests the existence of a relationship between altitude and STF; therefore, we attempted to quantify the impacts of altitude on the STF trends. Due to the uneven distribution of meteorological stations at different altitude levels, the altitude values (in 0.1 m) are processed with their logarithm. The FF trends as τ values were increased by 0.5, and then, the square root was taken to make the relationships between the FF trends and altitude clear.

Global climate change occurred in the 20th century

(Fu and Wang, 1992), which has been supported by many studies. Between 1985 and 2005, the San Juan Mountain region in southwestern Colorado experienced the most warming from 1990 (Lunagaria et al., 2011). The interannual variability of the western North Pacific western edge subtropical high in early summer experienced an interdecadal decrease around 1990 (Zhan et al., 2022), and North Pacific anomalous sea surface temperatures and atmospheric variability were more closely associated with the occurrence of the central Pacific El Niño after 1990 than before 1990 (Yeh et al., 2015). In Jiangsu, China, the decreasing reference evapotranspiration, which is an indicator of atmospheric evaporation capability, increased in the warming climate and showed a decreasing trend before 1990 but followed an increasing trend from 1990 to 2019 (Qin et al., 2021). The warming trend of air temperature in the Himalaya, in contrast to the global temperature, has been projected after 1990, with a greater warming rate in the maximum temperature than in the minimum temperature (Yadav et al., 2021). Across China, the rate of temperature increase peaked approximately 1990 (Appendix Fig. S2), which showed distinct warming patterns before and after 1990. Accordingly, we divide the time period into two parts, specifically, before 1990 and after 1990, to analyze the STF trends.

The Kriging interpolation that uses the 'gstat' package in R is applied to present the distributions and long-term trends of *FF* and *FA* (Bivand et al., 2008).

Phytoplankton are the primary producers in lakes and play an important role in biogeochemical cycling and the function of lake ecosystems (Reynolds et al., 1993; Cao et al., 2018). In their important role in lakes, phytoplankton have short life cycles and are sensitive to climate change, which makes phytoplankton an indicator of the climate impact on lake ecosystems (Liu et al., 2015). It has also been shown that an increase in surface water temperatures due to changing global climate could play a role in the proliferation of phytoplankton blooms (O'Neil et al., 2012). The relationship between phytoplankton blooms and STF can reflect the ecological effects of STF to a certain degree. The MODIS-Aqua data that we used to obtain the bloom area data in Taihu Lake (a highly eutrophic, large, shallow lake in eastern China, 30°55′40″N–31°32′58″N, 119°52′32″E–120°36′10″E) were acquired with a high frequency (1 image per day) from 2002 to 2019 and are freely available. These data have a maximum spatial resolution of 250 nm (the first two bands) and allow the monitoring of Taihu Lake over multiannual time periods at a medium resolution. The MODIS-Aqua level 0 data (raw digital counts) from 2003 to 2019 were obtained from the U.S. NASA Goddard Space Flight Center (GSFC, http://oceancolor.gsfc.nasa.gov/) (Shi et al., 2015). Extreme severe bloom events in 2007 and 2017 were caused by the weak wind in these years and the high total phosphorus concentration carried by the flood in the previous year (Zhu et al., 2019); therefore, these two years were excluded from the STF ecological analysis.

3 Results

3.1 Distributions of *FA* and *FF* in China

The short-term *FA* distributions had similar patterns among spring (March, April and May), autumn (September, October and November) and winter (December, January and February) (Fig. 2). The *FA* in the western part of China remained relatively low and stable among the seasons, while the *FA* values, which were high in the eastern part of China, changed in the three seasons. In spring (Fig. 2a), the *FA* values were higher in the eastern half than in the western half and had a maximum average value of 30.45°C/month nationwide. Conversely, the northern region showed a relatively high *FA*, except for in the summer (June, July and August). The mean *FA* was 23.91°C/month in the summer (Fig. 2b), which was the minimum among the seasons, and there was a minimum *FA* value of 7.35°C/month, which was also the minimum among the seasons. The *FA*s were quite uniform, except for a small region in Ningxia, which had a maximum *FA* value of approximately 61.02°C/month. In summer, most regions experienced a similar STF, and a sharp change in climate was rare. In autumn, with a 25.44°C/month mean *FA*, China seemed to be divided into three parts (Fig. 2c). The *FA*s were low in the western part, medium in the central part and high in the northeastern part. The *FA* in winter had an average value of 26.52°C/month, which was also divided into three parts (Fig. 2d). In a region near the eastern boundary of Yunnan, the *FA*s were significantly higher than those in the surrounding areas.

The *FF* distributions were different among the seasons and had similar patterns (Fig. 3). The regions with low *FF* distributions were located mainly in the north-

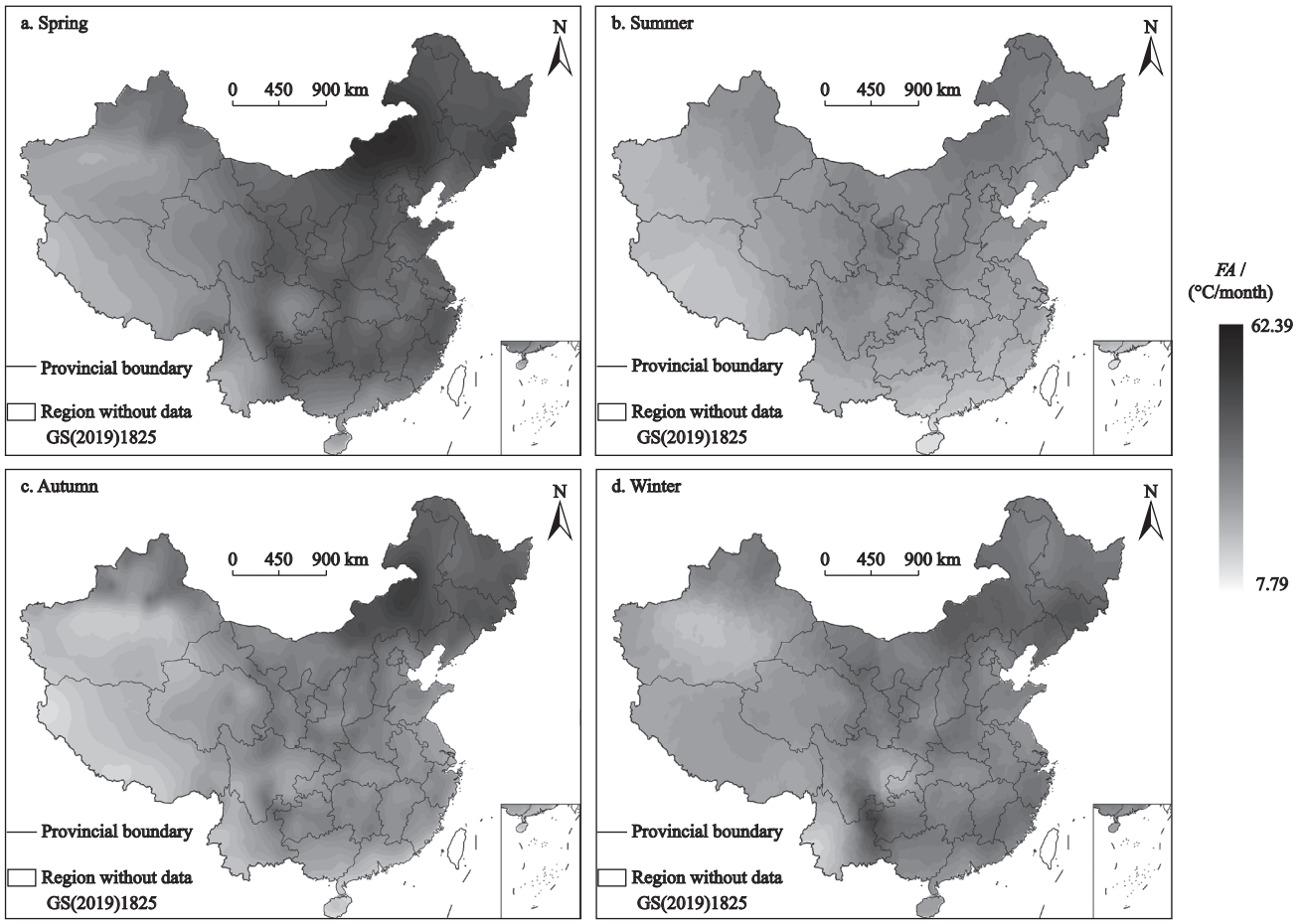

Fig. 2 Seasonal distributions of fluctuation amplitude (*FA*) in China

western and southern regions of China. Noticeably, Yunnan had the lowest *FF* in spring. The maximum value of the average *FF* was 5.72 d/month in summer, and the minimum value of the average *FF* was 5.33 d/month in winter. The *FF* distributions in spring and autumn were almost the same, with an average *FF* value of 5.62 d/month in spring and 5.51 d/month in autumn. The *FF* values in summer differed from the *FF* in spring and in autumn, and the distribution pattern also changed (Fig. 3b). The eastward migration of the low *FF* regions in the south caused a slightly different distribution pattern.

3.2 Trends of the *FA* and *FF* across China before 1990

The *FA* trend distributions across China before 1990 were different among seasons (Fig. 4). All average τ values in each season were negative, which indicates that the STF experienced a downward trend before 1990. The *FA* trend distributions were regional for the areas with positive or negative τ values that were well defined.

The *FA* trends before 1990 in spring decreased in most regions, as 64.24% of the stations had a negative τ value (Fig. 4a). The summer *FA* trends before 1990 had a maximum average τ value of –0.003 (Fig. 4b). A total of 57.80% of stations had positive τ values, while Xinjiang, part of Inner Mongolia, Hebei, Yunnan and Guangxi still had decreasing *FA* and *FF* trends. The *FA* trend distributions in autumn had 54.59% stations with negative τ values with very clear boundaries that divided the study area into the western, middle and eastern parts (Fig. 4c). The regions with increasing *FF* trends were in Tibet, southwestern China, and the southeastern coast, while regions with decreasing *FF* trends were distributed in the northern and middle regions of China. In winter, the *FA* trends for 73.46% of stations had negative τ values and a minimum τ value of 0.050 among the seasons. The *FA* distributions were also regional for the regions with increasing *FA* trends local-

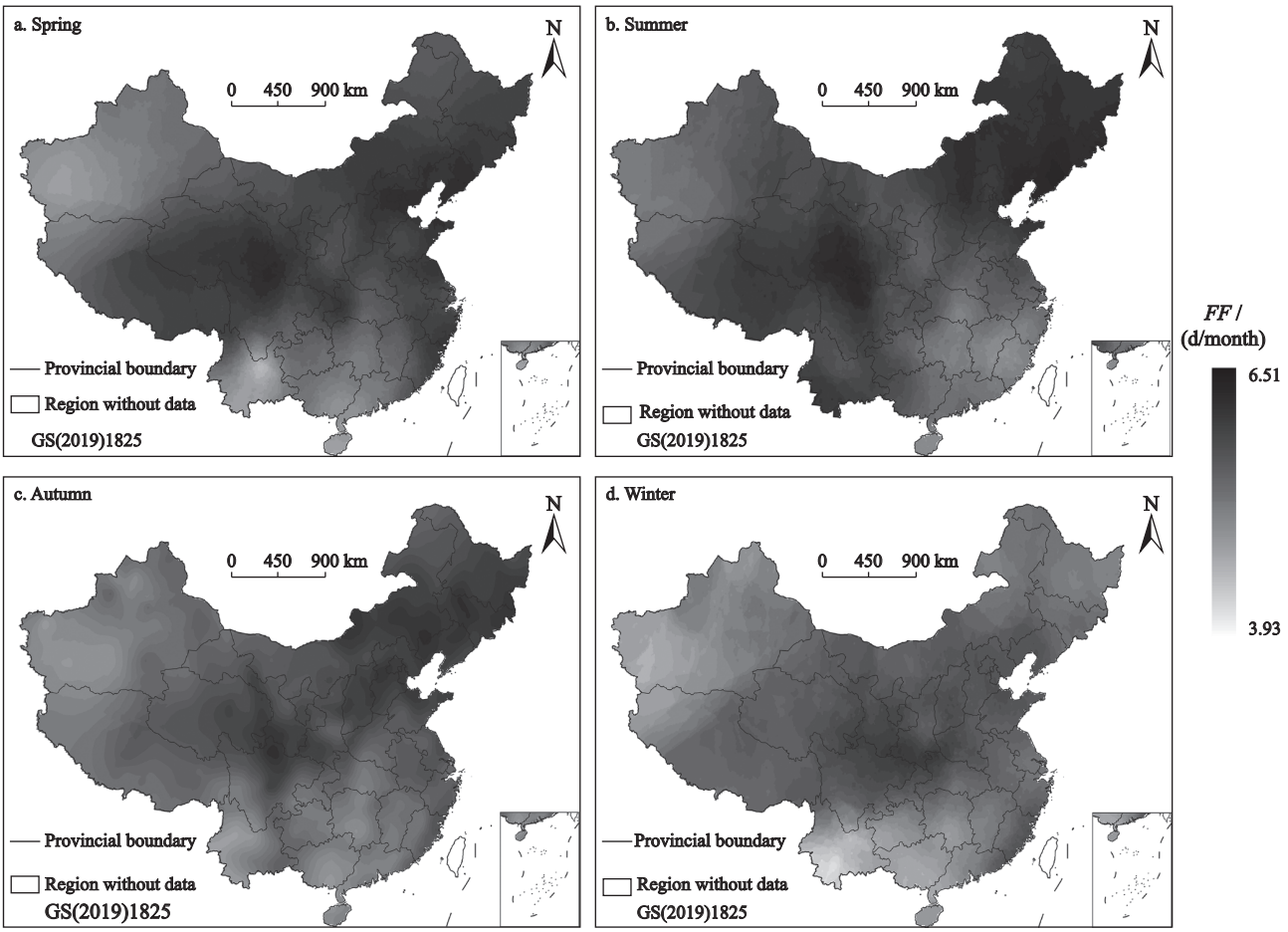

Fig. 3 Seasonal distributions of fluctuation frequency (*FF*) in China

ized in Tibet and northern Qinghai (Fig. 4d).

The *FF* trend distributions before 1990 were consistent with the *FA* trend distributions, while differences were found in the τ values (Fig. 5). The proportions of the stations with positive τ values of *FF* were 66.51%, 73.66%, 51.25% and 69.96% in spring, summer, autumn and winter, respectively.

3.3 Trends of the *FA* and *FF* across China after 1990

The *FA* trends after 1990 differed greatly in the distributions from the *FA* trends before 1990 (Figs. 6 and 7). Most regions had increasing *FA* trends among the seasons, and all average τ values were positive, which indicates that the STF trends increased after 1990. The *FA* trend distributions varied greatly among the seasons, which resulted in an obvious characteristic. The extreme points were obvious in the *FA* trend distributions after 1990.

In spring, regions with decreasing *FA* trends were present in the western and southern parts of China (Fig. 6a). The *FA* trends showed that 68.54% of the stations had positive τ values. In summer, regions with decreasing *FA* trends were present in the western and northeastern regions of China (Fig. 6b). A total of 74.16% of the stations in the summer had positive τ values. In autumn, the *FA* trends had the fewest stations with positive τ values, 49.44% (Fig. 6c). Regions with negative τ values were present in the southwestern and middle eastern parts. In winter, the *FA* trends had the second-highest number of stations with positive τ values, 70.79%. Regions in the northwest, northeast, and Yunnan areas had decreasing *FA* trends, which represented the smallest areas with negative τ values among the seasons (Fig. 6d).

The *FF* trends also presented almost the same distributions as the *FA* trends after 1990 (Fig. 7). The specific proportions of stations with positive τ values of *FF*

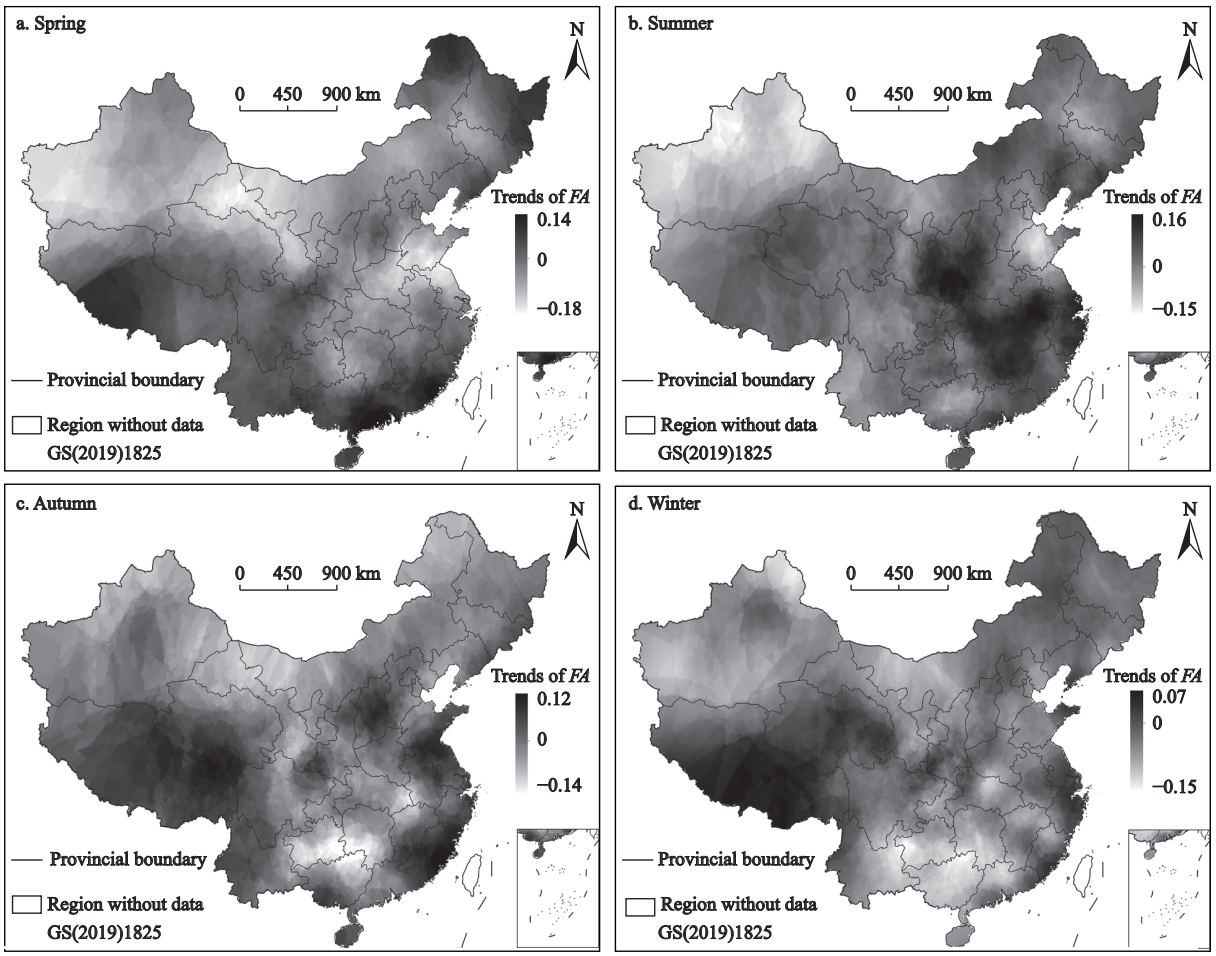

Fig. 4 Long-term fluctuation amplitude (*FA*) trend (τ, adjusted by the Mannkendall function) distributions in China before 1990. $\tau > 0$ indicates an increasing trend, and $\tau < 0$ indicates a deceasing trend. The absolute value of τ indicates the reliability of the trend

were 65.79%, 70.20%, 52.09% and 73.66% in spring, summer, autumn and winter, respectively.

3.4 Altitude effects on the *FA* and *FF* trends

The distributions of the *FA* and *FF* trends seemed to have a relationship with altitude. Therefore, we tried to uncover the altitude effects on the STF trends. The relationships between the *FA* and *FF* trends and altitude have the same patterns; thus, we show the variation in *FF* at different altitudes to represent the STF trend change with altitude in the two time periods (Fig. 8).

Before 1990, the *FF* trend in summer was influenced little by altitude, while in the other three seasons, the τ values of the *FF* trend changed with altitude in the two phases (Figs. 8a–d). In spring, the τ values increased with increasing altitude in the first phase, and the slope of the fitting line was lower in the second phase. In autumn and winter, the relationships between the *FF* trends and altitude showed similar patterns. In the first phase, the τ values decreased with increasing altitude, and the slope of the fitting lines increased in the whole second phase until the τ values were positively correlated with altitude. The two phases were divided by the logarithm of altitude equal to approximately 8.5 (the altitude values equaled approximately 500 m).

After 1990, the slope of fitting the line of the *FF* trend in spring changed several times. The slope of the fitting line was negative and stable when the logarithm of altitude was lower than 7.0 (altitude values lower than approximately 100 m). When the logarithm of altitude was 7.0–8.0 (the altitude value was approximately 100–300 m), the slope was positive and then close to 0 when the logarithm of altitude was 8.0–8.5 (the altitude value was approximately 300–500 m). The slope decreased again at an approximate logarithm of altitude equal to approximately 8.5 and then remained at a negative value in the higher altitude range. In summer, the slope of fitting was negative and decreased at a logar-

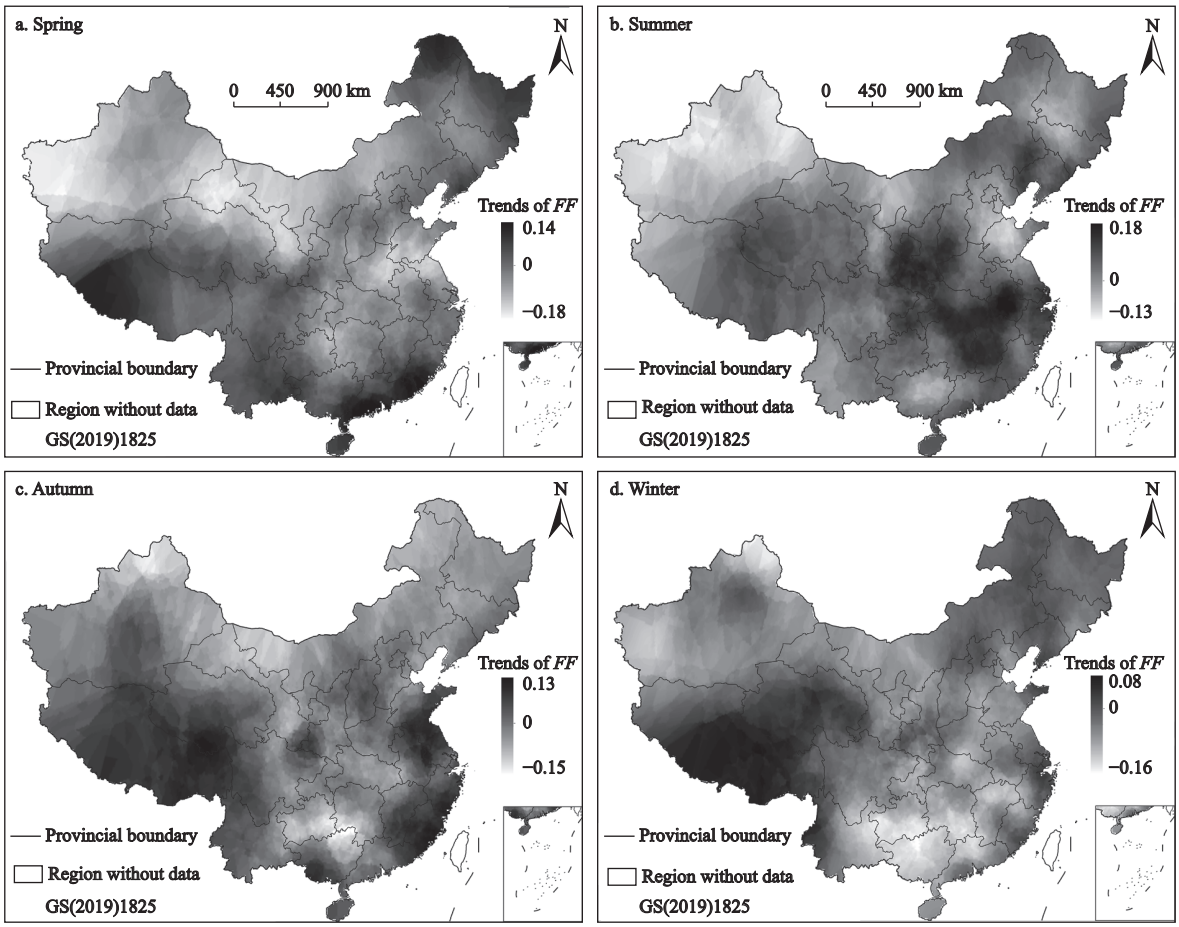

Fig. 5 Long-term fluctuation frequency (*FF*) trend (τ, adjusted by the Mannkendall function) distributions in China before 1990. $\tau > 0$ indicates an increasing trend, and $\tau < 0$ indicates a deceasing trend. The absolute value of τ indicates the reliability of the trend

ithm of altitude equal to approximately 9.9 (altitude value was approximately 2,000 m). In autumn the slope of the fitting line was positive and decreased at a logarithm of altitude equaled to approximately 8.5 until the slope was close to 0. In winter, the slope of the fitting line was close to 0and only positive at an approximate logarithm of altitude equal to 8.5.

3.5 Ecological effects of STFs

we utilize Taihu Lake as an example to couple the ecosystem and STFs in this study. The relationship between STFs and the bloom area in Lake Taihu (2003–2019, except for 2007 and 2017) reveals some ecological effects of STFs. A higher *FF* and *FA* in this season may result in a smaller bloom area in the following season (Fig. 9), although the correlations were weak.

Based on the correlation coefficient ranking, the STF in summer had the strongest correlation with the following autumn bloom area. The correlation between the winter STF and the following spring bloom area was weaker, and the relationships were too weak to confirm in the other two season pairs. The STF effects on the bloom area in the following season had no relevance to the air temperature because the air temperature did not have similar lag effects on the bloom area and was independent of seasonal *FF* and *FA*.

4 Discussion

4.1 Method evaluation

Our new method emphasizes the fluctuations in temperature over a period on the basis of eliminating the influence of season. The function of quantifying the STF amplitude and frequency improves the formulation of the STF.

Zhao used the ratio of the standard deviation to measure seasonal temperature fluctuations (Zhao et al., 2018). Meanwhile, our method focused on the temperat-

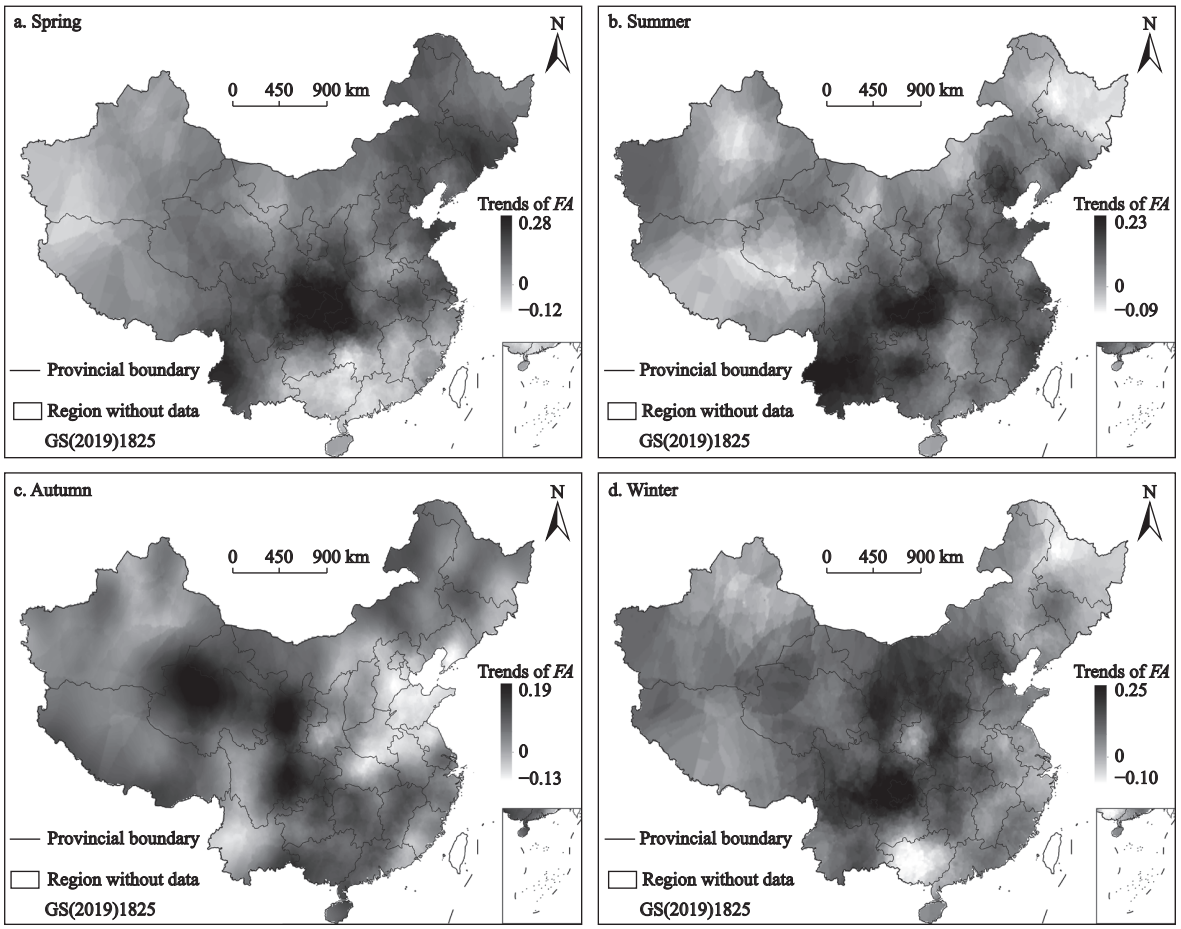

Fig. 6 Long-term fluctuation amplitude (*FA*) trend (τ, adjusted by the Mannkendall function) distributions in China after 1990. $\tau > 0$ indicates an increasing trend, and $\tau < 0$ indicates a deceasing trend. The absolute value of τ indicates the reliability of the trend

ure fluctuations in a specific time period (7 d) instead of daily temperature anomalies.

Qian quantified the intraseasonal weather fluctuations in eastern China by using EEMD, which could set timescales of several days to months (Qian et al., 2011). Both Qian's and our methods could measure the STF well, and we expanded the research area from eastern China to all of China. The *FA* and *FF* before and after 1990 also made the STF indicators more comprehensive.

Peng studied spring *FA* and *FF* form 1975−2015 and 1990−2015 and regarded a day as a 'fluctuation day' when the temperature difference between this day and the previous day was above 1°C (Peng et al., 2019). On the basis of Peng's research idea, our method extended the study period of STF to the whole year.

4.2 STF spatial distributions

Our results indicated that *FA* and *FF* varied spatially and temporally, with high *FA* and *FF* in eastern China in spring (Figs. 2 and 3). Our results also clearly indicated that the STF has changed during the last 60 years, with two apparent stages, i.e., the STF generally decreased before 1990 and increased after 1990. This could also be supported by the increase in extreme weather events due to global warming.

The topography of China could influence the variation in the distributions of *FA*. For instance, basins have relatively low *FA* values for STFs (Fig. 2). Such basin areas with low *FA* values were clear except in summer, when the STF was weak and the general *FA* values were low. A region with minimum *FA* can be identified in Xingjiang in northwestern China, where the Tarim Basin, the largest basin in China, is located. This banded basin has obvious boundaries in the south and north, where the Tianshan Mountains and Kunlun Mountains are. The Junggar Basin to the north and the Qaidam Basin to the southeast could also be identified according to the distributions of *FA*. Furthermore, the

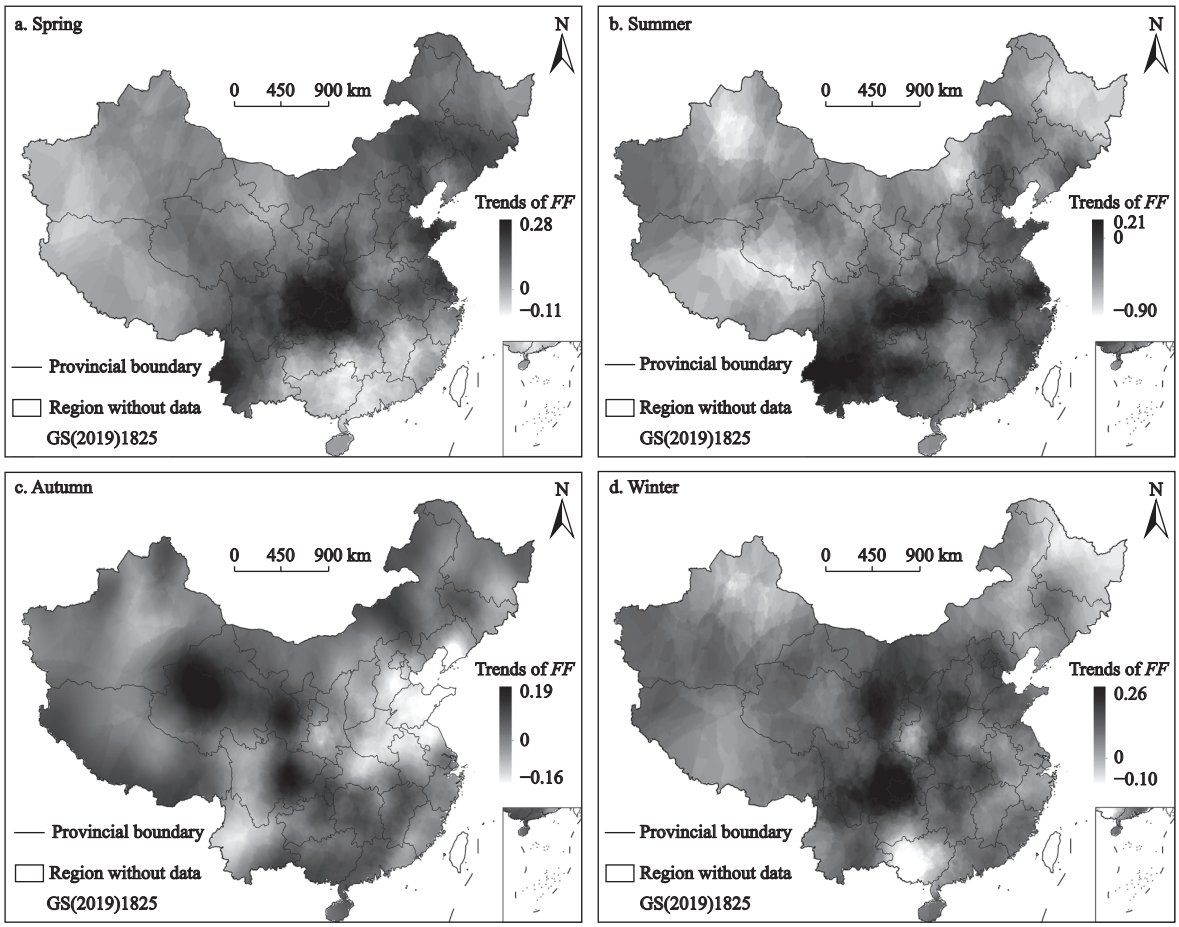

Fig. 7 Long-term fluctuation frequency (*FF*) trend (τ, adjusted by the Mannkendall function) distributions in China after 1990. $\tau > 0$ indicates an increasing trend, and $\tau < 0$ indicates the deceasing trend. The absolute value of τ indicates the reliability of the trend

location of the Sichuan Basin showed a circular region with low *FA* values, which could be easily identified in the spring. The Sichuan climate has been shown to have differences in the warming process and had a sudden change in precipitation in 1990, which confirms that its temperature fluctuation is specific and represents a reasonable division that occurred in 1990 (Chen et al., 2010). These consistencies in the distributions prove that the STF intensities in basins were quite low.

Mountains also contributed to the distributions of *FA*. For the mountains that bordered different terrains, the locations where the *FA* differences occurred coincided with the mountains in some cases (Figs. 1 and 2). In addition to the Tianshan Mountains and Kunlun Mountains mentioned above, the Hengduan Mountains and Qilian Mountains in the midwest are shown as yellow lines in *FA* distributions, which suggests that short-term temperatures fluctuate strongly in these two mountain regions. The northeast region, a region with high *FA* values, was divided by the Yinshan Mountains and the Great Hinggan Mountains. The Changbai Mountains along with a region on the east also showed higher *FA* values than the Northeast Plain to the east.

In the *FA* distributions, terrain plays a decisive role. Basins consistently have relatively low *FA* values, and mountain ranges sometimes correlate with changes in *FA*. Topographic features that interact with variation features, climatic conditions and other characteristics of a region determine the *FA* in this region (Ogwang et al., 2014). Regions with different topographical characteristics may exhibit different STF intensity characteristics.

Nationwide, the maximum *FF* occurred in summer, and the minimum indicators occurred in winter (Figs. 3b and d). This may indicate that the *FF* has a close relationship with the air temperature. However, when compared with the distribution of average temperature (Zhao et al., 2018), the regions with distinctively low-frequency indicators in the northwest and south do not ex-

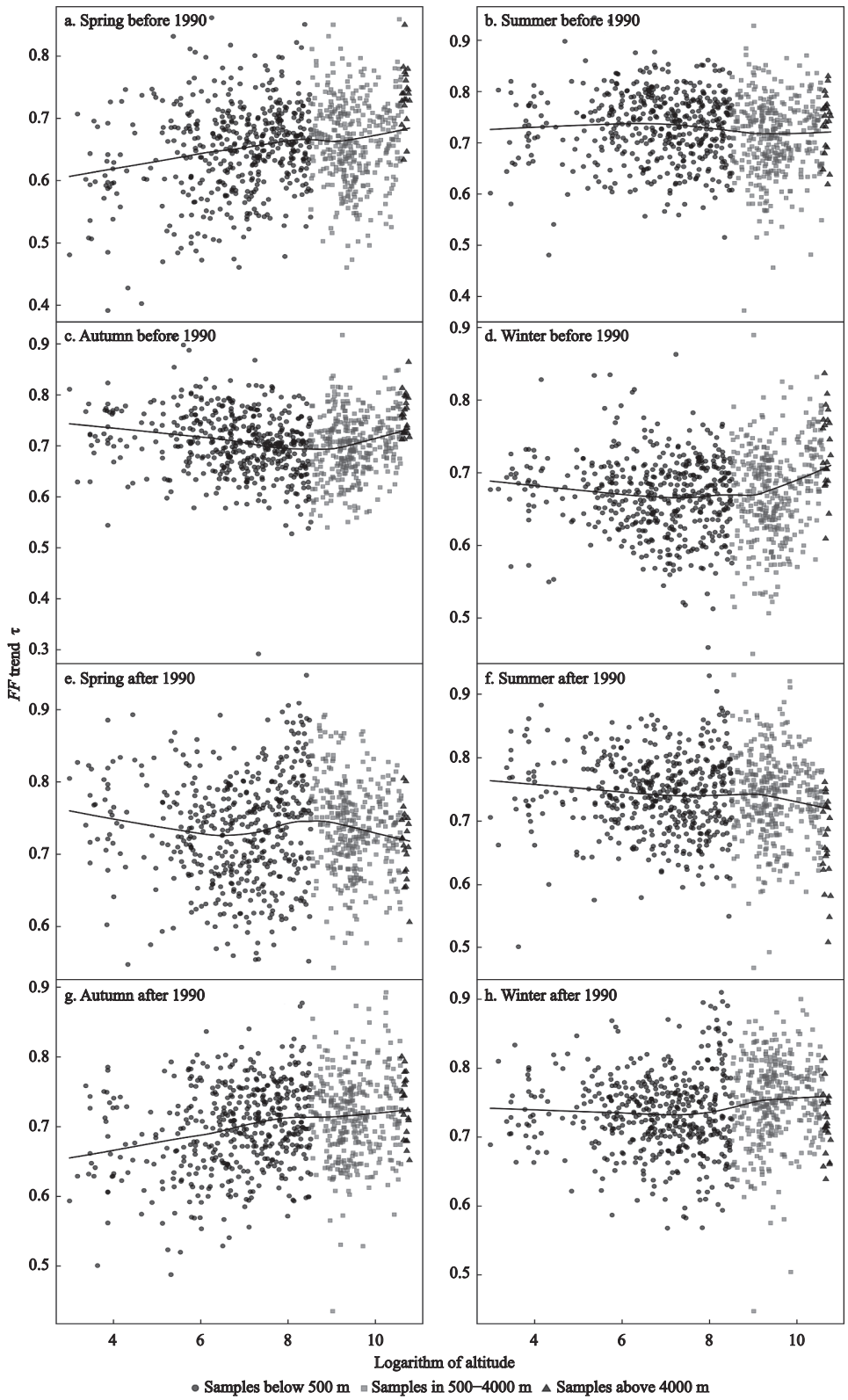

Fig. 8 Relationship between altitude and the fluctuation frequency (*FF*) trends (τ, adjusted by the Mannkendall function). The altitude values (0.1 m) were processed with their logarithm. The τ values of *FF* have were increased by 0.5, and then, the square root was taken. (a–d) seasonal relationships before 1990; (e–h) seasonal relationships after 1990. (a–d) and (e–h) are for spring, summer, autumn and winter. The samples are divided into three colors by the three steps of China's terrain (altitude below 500 m, 500 –4000 m and above 4000 m)

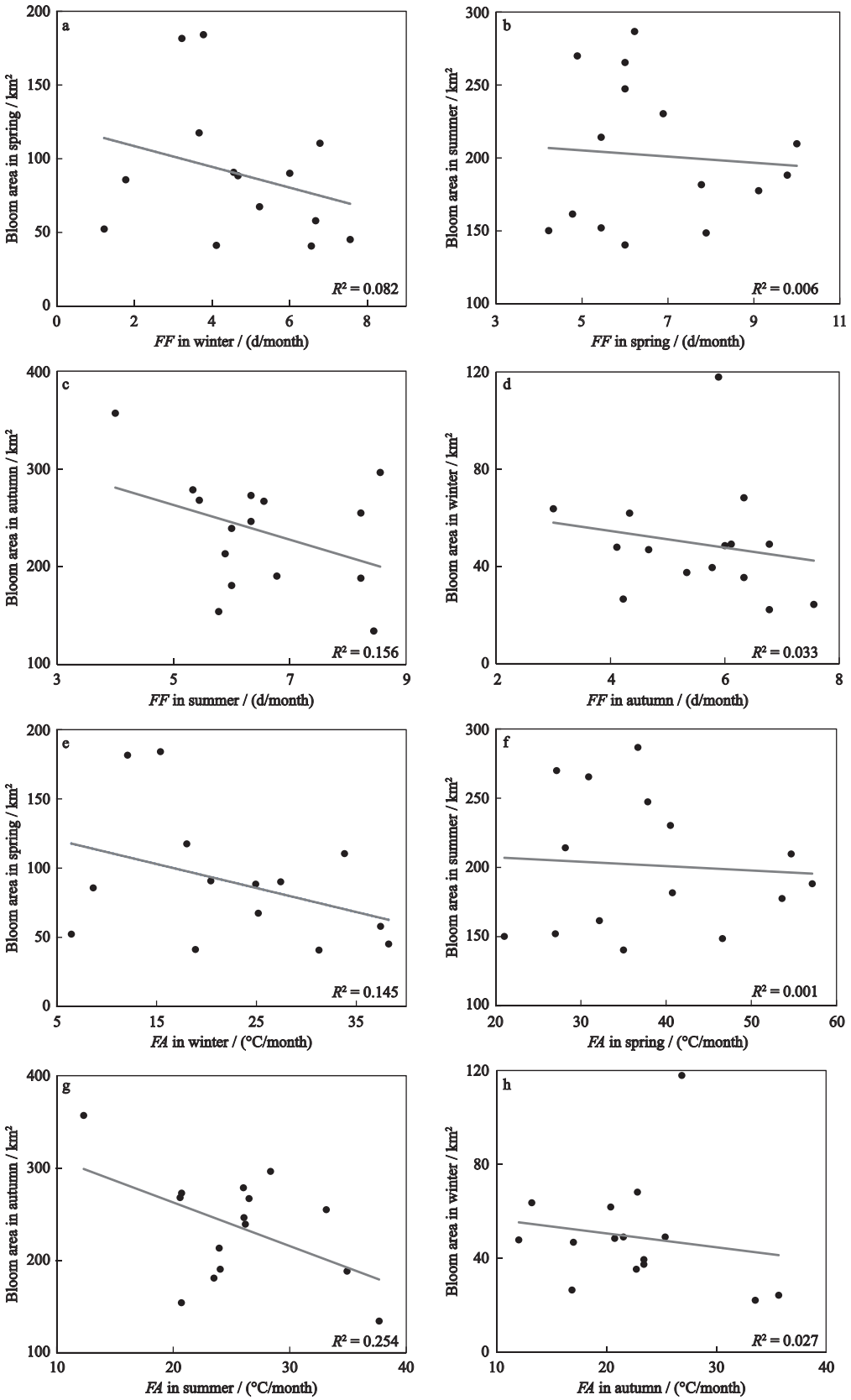

Fig. 9 Relationship between fluctuation frequency (*FF*) and fluctuation amplitude (*FA*) with the bloom area in Taihu Lake of China (2003–2019, except for 2007 and 2017). a–d are the relationships between *FF* and the bloom area in the seasons of winter-spring, spring-summer, summer-autumn and autumn-winter, respectively; e–h are the relationships between *FA* and the bloom area in the seasons of winter-spring, spring-summer, summer-autumn and autumn-winter, respectively

perience particularly low temperatures. Conversely, the coastal areas in the south have warmer climates than their surrounding regions. This phenomenon may prove that air temperature values do not directly determine the *FF*. For a specific region, climate processes may be associated with the *FF* of this region. A region may experience more frequent STF when it is comparative warm.

4.3 Long-term trends of the STF

The trend distributions of *FA* and *FF* were consistent with one another in the two time periods and might be forced by common factors, although their distributions had little in common (Figs. 4−7). The *FA* and *FF* trends before and after 1990 showed large differences in their distributions. In most situations before 1990, the *FA* and *FF* trends decreased, while the *FA* and *FF* trends increased after 1990, which has been identified in previous studies (Peng et al., 2019).

Before 1990, the *FA* and *FF* trends varied in the distribution among seasons, and the variation degree was weaker after 1990, thereby presenting a regional feature. Sorting by the size of the area under the increasing *FA* and *FF* trends, spring was ranked the lowest, followed by winter and autumn, and summer had the largest area of positive τ values. The *FA* and *FF* trend distributions had noteworthy characteristics in autumn (Figs. 4c and 5c). There were three independent regions with positive or negative τ values in autumn. Two of these regions are shown as red zones in the southwest and southeast, and another is shown as a blue zone in the north and middle part. The locations of these three regions were close to the altitude distributions when dividing the land into over 3000 m, between 500 m and 3,000 m, and below 500 m. The red zone in the southwest was the location of the Qinghai-Tibet Plateau, which averages over 4,000 meters above sea level and is in the category of over 3000 m, and it presented relatively high τ values, which does not occur only in autumn. The blue T-shaped part in the middle, including the Inner Mongolia Plateau and the Yunnan-Guizhou Plateau, was approximately in the 500 m to 3000 m range; the red part in the southeast corresponded to the range below 500 m. The Sichuan Basin, in the low altitude range, was in the region with increasing trends in fluctuations, as shown by a red region surrounded by the middle altitude range blue zone. The trend distributions had a high degree of overlap with the altitude distribution, and the altitude seemed to be a contributing factor to the changes in the temperature fluctuations. However, this relationship did not arise in other seasons, and the altitudes did not determine the τ values directly, which coincides with previous research on the relationship between altitude and temperature trends (Dong et al., 2015). The STF trends were regional and variable, and seasonal climate variations may be another factor that influenced them.

After 1990, the *FA* and *FF* trends for most regions increased, but their distributions were not as regional as before 1990 (Figs. 6 and 7). Although most regions that experienced similar *FA* and *FF* trends were localized, some regions with negative τ values were surrounded by regions with positive τ values. Compared with all the distributions above, the *FA* and *FF* trends after 1990 were the most varied because most regions had different *FA* and *FF* trends in different seasons, and the distributions showed little similarity with the *FA* and *FF* distributions or their trends. This may reveal that some strong forcing, probably related to the rapid urbanization after 1990 (Gu et al., 2012), occurred in approximately 1990 and made the STF experience a higher frequency and intensity than before. The poor stability of the *FA* and *FF* trends after 1990 revealed that these forces were more intensive than the topographical effects. Remarkably, the Qinghai-Xizang Plateau has distinct characteristics of STF, especially in *FA* and the STF trends before 1990, which may be due to its unique geography and climate conditions (Zheng, 1996).

4.4 Potential drivers of STFs

The variations in the STF trends along altitude had two different patterns, and they were divided at 500 m (the logarithm of altitude was approximately 8.5). The effects of altitude on the STF trends were different in plain areas (most plain areas are below 500 m in China) and higher altitude areas. Plain areas have their own climatic and underlying surface characteristics (Wu and Zheng, 2000), which results in the difference in the STF trend patterns between areas lower and higher than 500 m. Compared with spring and autumn, the STF trends were more weakly influenced by altitude, especially in summer. The sustained and relatively stable heat and cold in summer and winter might weaken the altitude contributions to STF trends.

The directions of the seasonal STF trends also changed differently before and after 1990: the STF trends increased in spring and decreased in autumn with increasing altitude overall before 1990, but they decreased in spring and increased in autumn after 1990; the STF trends remained in the same pattern in summer and winter, but the influence of altitude became weaker. These relationship changes revealed other stronger forces that affect the STF trends after 1990. Our hypothesis is that this force may be the accelerating urbanization after 1990. The expansion of built-up land was concentrated in eastern China, specifically, the southeast coastal areas and the plain region in the mainland, such as the Huang-Huai-Hai Plain, Yangtze River Delta, and Pearl River Delta (Liu et al., 2010). Previous researchers have also found that human influence produced a very large increase in the frequency of extremely hot summers and long-lasting severe heatwaves (Sun et al., 2014). In the Yangtze River Delta, rapid urbanization has even formed a 'heat island' phenomenon (Chen et al., 2003). Apparently, further research is needed to improve the relevance between human activities and STFs.

The underlying mechanism that dominates the STF is complex. The topography is only one of many controlling factors. The radiation budget can explain 79% of interannual temperature variability and 99% of the multidecadal temperature trends on land (Schwingshackl et al., 2018), which is considered a potential driver of STF. Arctic amplification acts to reduce subseasonal temperature variance (Screen, 2014), which indicates the potential contribution of atmospheric circulation to the STF. Our further studies will look forward to interpreting the mechanism of STF in more dimensions.

4.5 Ecological effects of STFs

Phytoplankton are sensitive to rapid temperature changes (Elliott et al., 2006), but studies on the effects of rapid temperature changes have mainly focused on temperature changes in one direction (increasing or decreasing). The relationship between the STF and bloom area in Lake Taihu could reflect some ecological effects of STFs, which measure the frequency and amplitude of rapid temperature changes.

Higher *FF* and *FA* values in winter and summer result in smaller bloom areas in the following spring and autumn. The negative effects of STFs on the bloom area are difficult to explain for its one-season delay. This correlation between STFs and phytoplankton may be driven by competition, which decreases the energy efficiency of phytoplankton among different phytoplankton species with different optimum temperature ranges (Laugaste et al., 2010). STFs may also affect phytoplankton through a strong carry-over effect on the phytoplankton community and biomass and on nutrient levels (Deng et al., 2020). The processes of how STFs affects phytoplankton development or other ecological processes are worth more research.

5 Conclusions

This research applies an original method to quantify STFs and analyzes the characteristics of seasonal spatial distributions and their trends in China. Our method can eliminate seasonal effects, which makes it applicable to different time scale (from days to years) STF analyses. The quantifications of *FA* and *FF* enrich the STF indicators, and the division of the research period reveals the STF change pattern more clearly. Short-term temperature experiences the most frequency and amplitude fluctuations in spring and the least in summer. The STF is weaker in autumn than in spring and in winter. The *FA* and *FF* distributions are greatly affected by topography. The *FA* and *FF* trends have identical distributions, which mainly increases before 1990 and decreasing after 1990. *FA* and *FF* trends had regional distributions before 1990 and had different distributions after 1990; in addition, these trends are more variable in the later period. The STF trends are more affected by altitude in spring and autumn than in summer and spring. The effects of altitude on the STF trends are weakened after 1990, which is probably related to human activities because the STF trend variations along altitude have their own patterns below 500 m, where urbanization is concentrated. The ecological effects of STFs are reflected by the one-season lag negative correlation between the STF and bloom area in Taihu Lake. Studies on this time range are quite limited; therefore, it is pertinent to research STFs in a 7-d range on a longer time period and larger space scales. Related experiments are also needed to identify more STF drivers and impacts.

Appendix

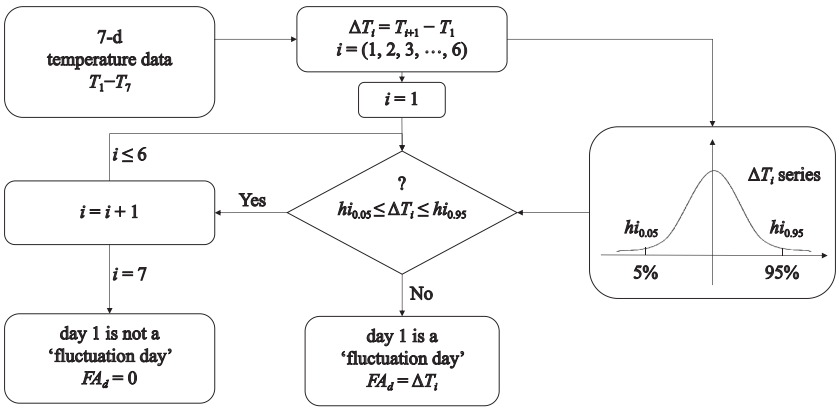

Fig. S1 Calculation flow chart to identify the fluctuations and measure FA_d. T_1 is the temperature of day 1, i corresponds to the number of days, T_{i+1} is the temperature of day i + 1, ΔT_i is the temperature difference between day 1 and day i + 1, ΔT_i of the same date in each year form the ΔT_i series, $hi_{0.05}$ is the 5% quantile of the ΔT_i series, $hi_{0.95}$ is the 95% quantile of the ΔT_i series, and FA_d is the FA value of the 'fluctuation day'

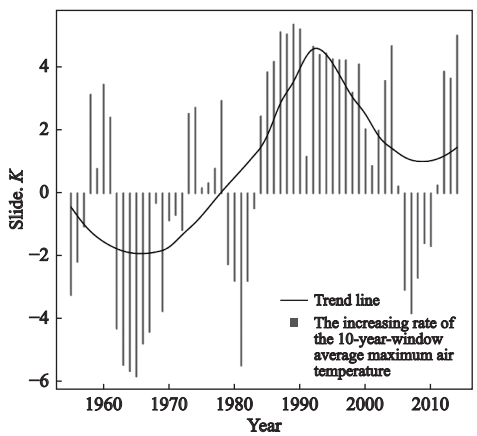

Fig. S2 Rate of increase in the air temperature across China. Slide. K is the increasing rate of the 10-year-window average maximum air temperature in China. For example, the Slide. K value of 2000 is the slope of the temperature linear fitting line from 1996 to 2005. The temperature data are the yearly average maximum temperature of all stations in China. The choice of the maximum temperature is consistent with the following analysis without affecting the results. The trend line is the curve fitted by the least absolute shrinkage and selection operator

References

Bivand R S, Pebesma E J, Gómez-Rubio V, 2008. *Applied Spatial Data Analysis with R*. New York: Springer.

Braganza K, Karoly D J, Arblaster J M, 2004. Diurnal temperature range as an index of global climate change during the twentieth century. *Geophysical Research Letters*, 31(13): L13217. doi: 10.1029/2004gl019998

Cao J, Hou Z Y, Li Z K et al. , 2018. Succession of phytoplankton functional groups and their driving factors in a subtropical plateau lake. *Science of the Total Environment*, 631 –632: 1127–1137. doi: 10.1016/j.scitotenv.2018.03.026

Chan W P, Chen I C, Colwell R K et al., 2016. Seasonal and daily climate variation have opposite effects on species elevational range size. *Science*, 351(6280): 1437–1439. doi: 10.1126/science.aab4119

Chen Chao, Pang Yanmei, Zhang Yufang, 2010. On the characteristics of climate change in Sichuan Basin in the recent 50 years. *Journal of Southwest University (Natural Science Edition)*, 32(9): 115–120. (in Chinese)

Chen J, Dai A G, Zhang Y C, 2019. Projected changes in daily variability and seasonal cycle of near-surface air temperature over the globe during the twenty-first century. *Journal of Climate*, 32(24): 8537–8561. doi: 10.1175/JCLI-D-19-0438.1

Chen Longxun, Zhu Wenqin, Zhou Xiuji et al., 2003. Characteristics of the heat island effect in Shanghai and its possible mechanism. *Advances in Atmospheric Sciences*, 20(6): 991–1001. doi: 10.1007/BF02915522

Deng J M, Zhang W, Qin B Q et al., 2020. Winter climate shapes spring phytoplankton development in non-ice-covered lakes: subtropical Lake Taihu as an example. *Water Resources Research*, 56(9): e2019WR026680. doi: 10.1029/2019WR026680

Dong D H, Huang G, Qu X et al., 2015. Temperature trend-altitude relationship in China during 1963−2012. *Theoretical & Applied Climatology*, 122(1): 285–294. doi: 10.1007/s00704-014-1286-9

Eichner J F, Koscielny-Bunde E, Bunde A et al., 2003. Power-law persistence and trends in the atmosphere: a detailed study of long temperature records. *Physical Review E*, 68(4): 046133. doi: 10.1103/PhysRevE.68.046133

Elliott J A, Jones I D, Thackeray S J, 2006. Testing the sensitivity of phytoplankton communities to changes in water temperature and nutrient load, in a temperate lake. *Hydrobiologia*,

559(1): 401–411. doi: 10.1007/s10750-005-1233-y

Fu Congbin, Wang Qiang, 1992. The definition and detection of the abrupt climatic change. *Scientia Atmopherica Sinica*, 16(4): 482–493. (in Chinese)

Gu C L, Wu L Y, Cook I, 2012. Progress in research on Chinese urbanization. *Frontiers of Architectural Research*, 1(2): 101–149. doi: 10.1016/j.foar.2012.02.013

IPCC, 2021. *Climate Change 2021: The Physical Science Basis. Contribution of Working Group I to the Sixth Assessment Report of the Intergovernmental Panel on Climate Change*. Cambridge: Cambridge University Press.

Jang Y S, Shen S F, Juang J Y et al., 2022. Discontinuity of diurnal temperature range along elevated regions. *Geophysical Research Letters*, 49(6): e2021GL097551. doi: 10.1029/2021gl097551

Karl T R, Knight R W, Plummer N, 1995. Trends in high-frequency climate variability in the twentieth century. *Nature*, 377(6546): 217–220. doi: 10.1038/377217a0

Kilham S S, 1987. Phytoplankton ecology: structure, function and fluctuation. *Trends in Ecology & Evolution*, 2(12): 380. doi: 10.1016/0169-5347(87)90143-1

Lambrechts L, Paaijmans K P, Fansiri T et al. , 2011. Impact of daily temperature fluctuations on dengue virus transmission by *Aedes aegypti*. *Proceedings of the National Academy of Sciences of the United States of America*, 108(18): 7460–7465. doi: 10.1073/pnas.1101377108

Laugaste R, Haberman J, Blank K, 2010. Cool winters versus mild winters: effects on spring plankton in Lake Peipsi. *Estonian Journal of Ecology*, 59(3): 163–183. doi: 10.3176/eco.2010.3.01

Liu Jiyuan, Zhang Zengxiang, Xu Xinliang et al., 2010. Spatial patterns and driving forces of land use change in China during the early 21st century. *Journal of Geographical Sciences*, 20(4): 483–494. doi: 10.1007/s11442-010-0483-4

Liu L M, Yang J, Lv H et al., 2015. Phytoplankton communities exhibit a stronger response to environmental changes than bacterioplankton in three subtropical reservoirs. *Environmental Science & Technology*, 49(18): 10850–10858. doi: 10.1021/acs.est.5b02637

Liu Q, Tan Z M, Sun J et al., 2020. Changing rapid weather variability increases influenza epidemic risk in a warming climate. *Environmental Research Letters*, 15(4): 044004. doi: 10.1088/1748-9326/ab70bc

Lunagaria M M, Patel H R, Shah A V et al., 2011. Validation of PRECIS baseline (1961-1990) simulation for middle Gujarat agroclimatic zone. *Journal of Agrometeorology*, 13(2): 92–96.

Meis S, Thackeray S J, Jones I D, 2009. Effects of recent climate change on phytoplankton phenology in a temperate lake. *Freshwater Biology*, 54(9): 1888–1898. doi: 10.1111/j.1365-2427.2009.02240.x

Ogwang B A, Chen H S, Li X et al., 2014. The influence of topography on East African October to December climate: sensitivity experiments with RegCM4. *Advances in Meteorology*, 2014: 143917. doi: 10.1155/2014/143917

O'Neil J M, Davis T W, Burford M A et al., 2012. The rise of harmful cyanobacteria blooms: the potential roles of eutrophication and climate change. *Harmful Algae*, 14: 313–334. doi: 10.1016/j.hal.2011.10.027

Peces M, Astals S, Mata-Alvarez J, 2013. Response of a sewage sludge mesophilic anaerobic digester to short and long-term thermophilic temperature fluctuations. *Chemical Engineering Journal*, 233: 109–116. doi: 10.1016/j.cej.2013.07.088

Peng Kai, Deng Jianming, Zhang Yunlin et al., 2019. Short-term temperature fluctuation in the spring in China during 1957-2015. *Climatic and Environmental Research*, 24(1): 125–134. (in Chinese)

Qian Cheng, Yan Zhongwei, Wu Zhaohua et al., 2011. Trends in temperature extremes in association with weather-intraseasonal fluctuations in eastern China. *Advances in Atmospheric Sciences*, 28(2): 297–309. doi: 10.1007/s00376-010-9242-9

Qin M S, Zhang Y, Wan S Q et al., 2021. Impact of climate change on "evaporation paradox" in province of Jiangsu in southeastern China. *PLoS One*, 16(2): e0247278. doi: 10.1371/journal.pone.0247278

R Core Team, 2020. R: a language and environment for statistical computing. R Foundation for Statistical Computing, Vienna, Austria. https://www.R-project.org/

Reynolds C S, Padisák J, Sommer U, 1993. Intermediate disturbance in the ecology of phytoplankton and the maintenance of species diversity: a synthesis. *Hydrobiologia*, 249(1): 183–188. doi: 10.1007/BF00008853

Salmaso N, Naselli-Flores L, Padisák J, 2015. Functional classifications and their application in phytoplankton ecology. *Freshwater Biology*, 60(4): 603–619. doi: 10.1111/fwb.12520

Schwingshackl C, Hirschi M, Seneviratne S I, 2018. Global contributions of incoming radiation and land surface conditions to maximum near-surface air temperature variability and trend. *Geophysical Research Letters*, 45(10): 5034–5044. doi: 10.1029/2018GL077794

Screen J A, 2014. Arctic amplification decreases temperature variance in northern mid- to high-latitudes. *Nature Climate Change*, 4: 577–582. doi: 10.1038/NCLIMATE2268

Shi K, Zhang Y L, Zhu G W et al., 2015. Long-term remote monitoring of total suspended matter concentration in Lake Taihu using 250 m MODIS-Aqua data. *Remote Sensing of Environment*, 164: 43–56. doi: 10.1016/j.rse.2015.02.029

Shine R, Elphick M J, 2001. The effect of short-term weather fluctuations on temperatures inside lizard nests, and on the phenotypic traits of hatchling lizard. *Biological Journal of the Linnean Society*, 72(4): 555–565. doi: 10.1006/bijl.2000.0516

Singsaas E L, Sharkey T D, 1998. The regulation of isoprene emission responses to rapid leaf temperature fluctuations. *Plant, Cell & Environment*, 21(11): 1181–1188. doi: 10.1046/j.1365-3040.1998.00380.x

Sulastri, Henny C, Santoso A B, 2019. Phytoplankton composition and the occurrence of cyanobacterial bloom in Lake Maninjau, Indonesia. *IOP Conference Series Earth and Environmental Science*, 380: 012020. doi: 10.1088/1755-1315/380/1/

012020

Sun Y, Zhang X B, Zwiers F W et al., 2014. Rapid increase in the risk of extreme summer heat in Eastern China. *Nature Climate Change*, 4(12): 1082–1085. doi: 10.1038/nclimate2410

Wu Shaohong, Zheng Du, 2000. New recognition on boundary between tropical and subtropical zone in the middle section of eco-geographic system. *Acta Geographica Sinica*, 55(6): 689–697. (in Chinese)

Yadav J S, Tiwari S K, Misra A et al., 2021. High-altitude meteorology of Indian Himalayan Region: complexities, effects, and resolutions. *Environmental Monitoring and Assessment*, 193(10): 654. doi: 10.1007/s10661-021-09418-y

Yeh S W, Wang X, Wang C Z et al., 2015. On the relationship between the North Pacific climate variability and the Central Pacific El Niño. *Journal of Climate*, 28(2): 663–677. doi: 10.1175/jcli-d-14-00137.1

Yin Y H, Ma D Y, Wu S H et al., 2017. Nonlinear variations of forest leaf area index over China during 1982-2010 based on EEMD method. *International Journal of Biometeorology*, 61(6): 977–988. doi: 10.1007/s00484-016-1277-x

Zhan H Y, Chen R D, Lan M, 2022. Interdecadal change in the interannual variation of the western edge of the Western North Pacific subtropical high during early summer and the influence of tropical sea surface temperature. *Journal of Tropical Meteorology*, 28(1): 57–70. doi: 10.46267/j.1006-8775.2022.005

Zhan Z Y, Zhao Y, Pang S J et al. , 2017. Temperature change between neighboring days and mortality in United States: a nationwide study. *Science of the Total Environment*, 584–585: 1152–1161. doi: 10.1016/j.scitotenv.2017.01.177

Zhao C L, Chen J G, Du P et al., 2018. Characteristics of climate change and extreme weather from 1951 to 2011 in China. *International Journal of Environmental Research & Public Health*, 15(11): 2540. doi: 10.3390/ijerph15112540

Zheng Du, 1996. The system of physico-geographical regions of the Qinghai-Xizang (Tibet) Plateau. *Science in China Series D: Earth Science)*, 39(4): 410–417. (in Chinese)

Zhu Wei, Chen Huaimin, Wang Ruochen et al., 2019. Analysis on the reasons for the large bloom area of Lake Taihu in 2017. *Journal of Lake Sciences*, 31(3): 621–632. (in Chinese). doi: 10.18307/2019.0302